Comprehensive Telerobotic Ultrasound System for Abdominal Imaging: Development and *in-vivo* Feasibility Study

Deepak Raina[1*], Hardeep Singh[2], Subir Kumar Saha[1], Chetan Arora[1], Ayushi Agarwal[3], Chandrashekhara SH[3], Krithika Rangarajan[3], Suvayan Nandi[2]

***Abstract*— During the COVID-19 pandemic, the lives of healthcare professionals are at significant threat because of the enormous workload and cross-infection risk. Ultrasound (US) imaging plays a vital role in the diagnosis and follow-up of COVID-19 patients; however, it requires a close-physical contact by the sonographer. In this context, this paper presents a Telerobotic Ultrasound (TR-US) system for complete remote control of the US probe, thereby preventing direct physical contact between patients and sonographers. The system consists of a 6-DOF robot arm at the remote site and a haptic device at the doctor's site. The control architecture precisely transmits the intended position and orientation of the US probe to the remote location for transversal and sagittal plane scanning. This architecture, when integrated with an admittance controller-based force modulation and feedback transmission, enables the radiologists to obtain high-quality images for diagnosis. The advantages and effectiveness of the system are demonstrated by conducting *in-vivo* feasibility study at AIIMS, Delhi, for imaging abdomen organs (liver, spleen, kidneys, bladders). The system provides image quality equivalent to a manually-guided probe, can identify various pathology and reports high acceptability among volunteers and doctors from a questionnaire survey.**

I. Introduction

The second wave of COrona VIrus Disease 2019 (COVID-19) has wreaked havoc in India, with a catastrophic rise in the numbers of new infections in April and May. As of June 4, 2021, the country has recorded over 28.6 million cases and over 3,40,719 fatalities [1]. Healthcare facilities and staff across the country are struggling to cope up with the surge in cases due to the spread of infection among doctors, nurses and paramedics [2]. The prevailing situation has impacted regular health care services, especially those involving direct physical contact with the patient.

The healthcare community has significant evidence that Ultrasound (US) imaging plays a vital role in the diagnosis of a wide variety of diseases including COVID-19. It provides an essential framework for the management of these diseases and developing effective treatment strategies [3]–[5]. However, several concerns need to be addressed for US imaging during the COVID-19 pandemic. The US scanning procedure requires close physical contact between the doctors and patients, which puts them at risk of virus transmission. Moreover, there have been infected cases reported even with Personal Protective Equipments (PPEs) in some cases [6]. Therefore preventing infection among doctors due to the close-contact ultrasound procedure has become an urgent problem to be solved.

*Corresponding author deepak.raina@mech.iitd.ac.in, [1]Indian Institute of Technology, Delhi, India; [2]Addverb Technologies, Noida, India; [3]All India Institute of Medical Sciences, Delhi, India

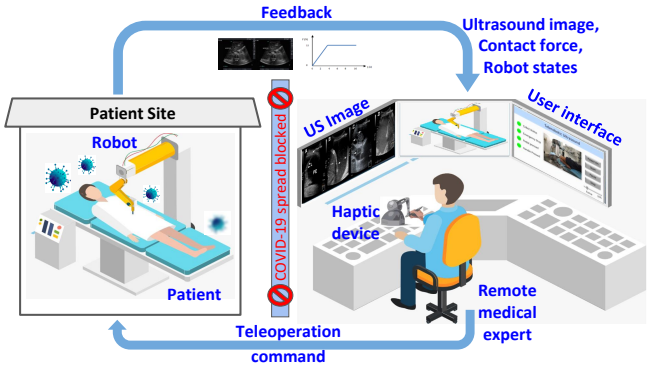

Fig. 1: Schematic of the developed Telerobotic Ultrasound system for abdominal imaging during COVID-19 pandemic

More robots on the front lines limit person-to-person contact and hence lower the risk of infection among healthcare workers [7]. Robots can also reduce the consumption of PPEs and prevent community transmission. However, US imaging is an operator-dependent modality and obtaining accurate images depends on the skill of the sonographer. Thus, the telerobotic solution seems to be a reasonable and promising direction, which allows the expert sonographer or radiologist to remotely manipulate a probe attached to the robotic system and generate images in real-time. This will ensure the safety of patients as well as doctors [8]. The people in rural areas will also benefit from this technology by getting examined by the expert doctors available in the urban areas.

The use of telerobotics in ultrasound applications has gained a lot of researchers' attention. Initially, the focus was on developing custom-designed robots to meet the technical requirements of ultrasound procedures [9], [10]. However, these systems could not meet all patient safety requirements, such as automated collision avoidance, force sensitivity, and mechanical safety features. Later on, with the availability of commercial robotic manipulators meeting the safety requirements of physical human-robot interaction, the focus of the research community shifted towards developing advanced control algorithms to achieve smooth and robust teleoperation [11]–[13]. During the COVID-19 pandemic, several teleoperated systems have been proposed and tested for ultrasound imaging. The study by [14] used the commercial telerobotic ultrasound system named MGIUS-R3 with 5G connectivity for the ultrasound imaging of heart and lungs of COVID-19 patients, where the system successfully evaluated lung lessions and precardial effusions in patients [14], [15]. However, the system has limited control capabilities and does

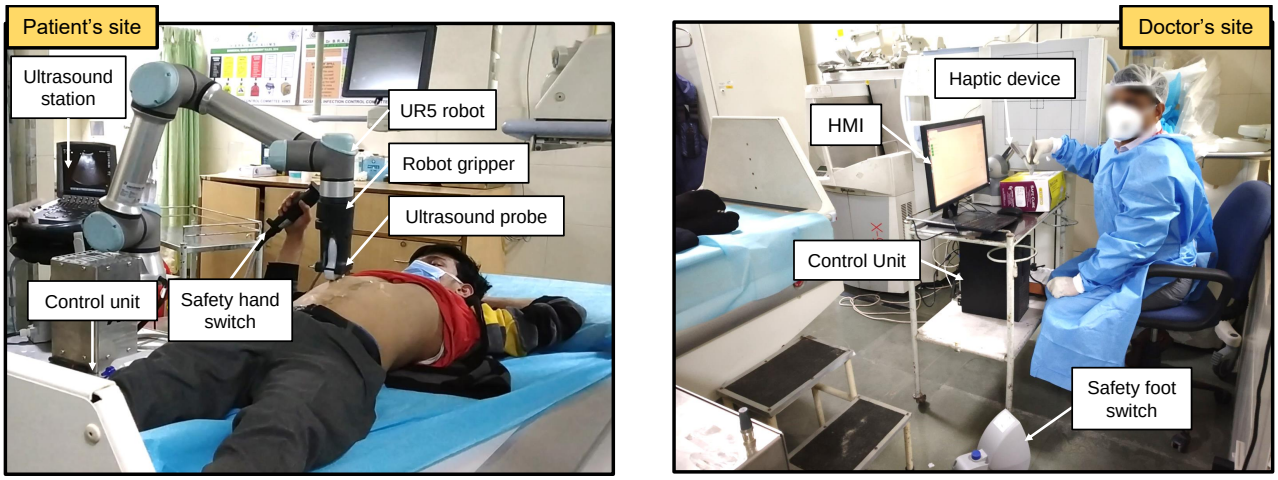

Fig. 2: Telerobotic ultrasound (TR-US) system at AIIMS, Delhi, during the COVID-19 pandemic. The volunteer is undergoing abdominal US while the doctor, sitting at a safe distance (>6 feet) from the patient, manipulates the haptic device's stylus to control the precise movements of the US probe attached to the robot's end-effector.

not allow doctors to vary the force and sense its feedback. MELODY is another commercial system, which comprises a custom-designed robotic probe holder and requires an assistant at patient site to handle the coarse translation and pressure modulation, while expert sonographer controls the orientation of probe. This system has been tested for several ultrasound examinations in more than 300 patients [16]–[18].

The above-discussed solutions permit limited degrees-of-freedom of the probe, require the presence of atleast one healthcare worker in close vicinity of the patient and focused on single organ scanning [19]. In this paper, we present a Telerobotic Ultrasound (TR-US) system for imaging abdomen organs which provides comprehensive control and perception of the US probe, equivalent to the manually operated procedure. The aforementioned works show significant progress in the field; however, to the best of our knowledge, a complete telerobotic system for scanning abdomen organs has seldom been reported. TR-US of abdomen is challenging due to the large number of organs, which require multiple scans at complex poses of the probe with varying pressure for accurate diagnosis. In our TR-US system, the controller transmits the 6D pose of the US probe to a remote site while ensuring smooth and vibration-free motion. The controller is integrated with a variable force control to get good quality images while ensuring the safety of patients. The doctor at a distant site will also get the feedback of pressure being applied on the patient's body. In addition, the system does not require the presence of auxiliary staff at the remote site during the procedure, except for the initial application of a coupling agent for a small duration.

To demonstrate the system's feasibility, we conducted an abdominal ultrasound test on human subjects at All India Institute of Medical Sciences (AIIMS), Delhi, where we compared the images obtained from our system with the hand guidance of the probe. A comprehensive satisfaction survey has also been conducted to get the feedback of system from doctors and volunteers. This paper is organized as follows: Section II describes the hardware architecture of TR-US system. Section III describes the control architecture for this system and its sub-components. Finally, the experiments and results are presented in Section IV for the volunteer trials at AIIMS. Conclusion and future works are discussed in Section V.

II. Telerobotic Ultrasound (TR-US) System

The developed TR-US system, shown in Fig. 2, consists of a UR5 collaborative robotic manipulator by Universal Robots, Denmark, at the patient site with an inbuilt force sensor. The US probe is attached to its end-effector using the custom-designed gripper. The sonographer manipulates the probe using the Geomagic haptic touch device by 3D Systems, USA while observing the continuous feed of US images on the Sonosite M-TURBO model screen.

A. Control Unit

The system uses two control units, one at the patient's site and one at the doctor's site. The control unit at the doctor's site has a Central Processing Unit (CPU) with QuadCore Intel i5-960 3.2 GHz processor, 8 GB of RAM, and is running on Linux Ubuntu 16.04 OS. The control unit at the patient site has a robot controller, battery and WiFi router, as shown in Fig. 3a. The Ultralife lead-acid battery has been used to provide power backup to the robot so that it can also carry its operation in a region where a power supply is not available. The whole controller unit and robot have been mounted on a mobile platform so that it becomes easy to maneuver it to perform bedside examinations in an isolation ward of COVID-19.

B. Human-Machine Interface (HMI)

HMI is provided at the doctor's site, which allows the doctor to communicate with the control unit at the patient's site, as shown in Fig. 3b. It will help a doctor to modulate the force being exerted on the patient's body using the slider bar. The live streaming of the patient site is also provided so that doctors can monitor the movements of the probe and the patient's response to the examination.

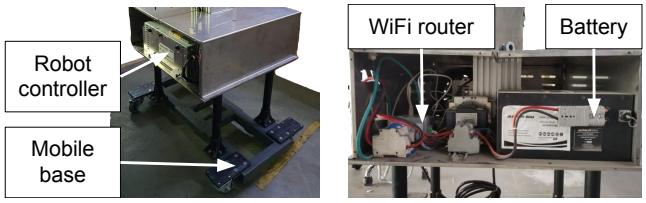

(a) Control unit at patient site

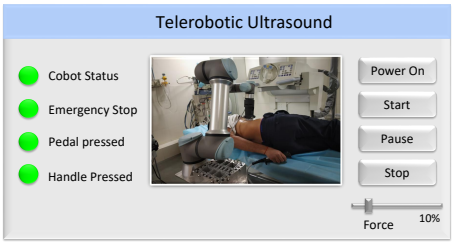

(b) Human-Machine Interface (HMI)

(c) Gripper

Fig. 3: Hardware components of TR-US

C. US Probe Gripper

The novel gripper has been designed to hold a range of US probes like linear and curvilinear, as shown in Fig 3c. The attendant at the patient's site can use this gripper to attach, detach, and change the probe as needed.

D. Safety Systems

The system has multiple protection measures to ensure the patient's safety: (1) an emergency stop button is installed next to the robotic arm (2) the controller has joint velocity limits (3.2 rad/s) and force limit (0-20 N) settings; and (3) a switch in the patient's hand and the pedal near the doctor's foot to stop the robotic arm.

III. Control Architecture of TR-US

When the ultrasound examination starts, the robot will start moving in a vertically downward direction until the probe touches the patient's body and becomes stable at a contact force of 2N. The teleoperation mode gets activated using a grey button on the haptic device's stylus. Abdominal ultrasound requires scanning a large region of the body while maintaining complex probe orientations, which are difficult to achieve while the probe is in contact with the body. In such cases, doctors can press the white button to pull the probe away from the patient's body at a predefined height, allowing him to conveniently change the probe's pose. The steps of the TR-US control program have been given in Algorithm 1, which uses a Robot Operating system (ROS) and Socket-based interface to communicate with haptic device and robot, respectively. The controller has two components: Motion mapping and Force control.

A. Motion mapping

The motion mapping strategy has been devised to tele-operate the UR5 robotic arm using a haptic device. The mapping of workspace must be formulated intuitively and efficiently [20], so that doctors can quickly learn to control the fine movements of the probe remotely using the haptic

Algorithm 1 Control algorithm for TR-US

Input: Haptic device's stylus movement by the sonographer
Output: Movement of ultrasound probe at the patient site

Initialization
while *not connected* **do**
    connected ← socket_open(ip_address, port_id)
end while
$[\boldsymbol{p}^r, \boldsymbol{o}^r, \boldsymbol{f}^r]_{t-1}$ ← RobotState()
$[\boldsymbol{p}^g, \boldsymbol{o}^g]_{t-1}$, $[\boldsymbol{p}^g, \boldsymbol{o}^g]_t$ ← GeomagicState()
$[\boldsymbol{p}^r, \boldsymbol{o}^r, \boldsymbol{f}^g]_t$ ← Mapping()
while *white_button is not pressed* **do**
    force_mode(des_force=2)
    if *grey_button is pressed* **then**
        target ← $[\boldsymbol{p}^r, \boldsymbol{o}^r]_t$
        force_feedback($\boldsymbol{f}^g_t$)
    end if
    MoveTo(target)
end while
while *white_button is pressed* **do**
    end_force_mode()
    target ← $[\boldsymbol{p}^r, \boldsymbol{o}^r]_t$
    MoveTo(target)
end while

device. Though joint space mapping is the most common method, we chose task space-based mapping as our system is subjected to force constraints in task space. It becomes quite difficult to satisfy such constraints while planning in joint space. On the other hand, task-space mapping can reliably control both position and force. Moreover, it is intuitive and can be easily adopted by the user. The flow chart of implemented motion mapping controller is shown in Fig. 4. To map the devices in task space, first, the DH parameters

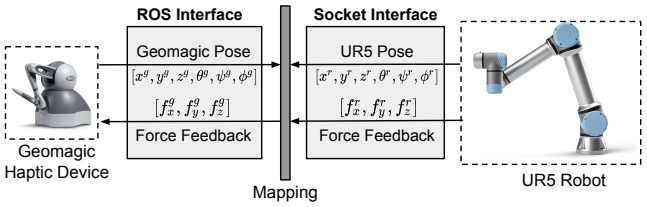

Fig. 4: Flow chart of motion-mapping controller

of the Geomagic haptic touch device have been identified as shown in Table I, while the UR5 robot's parameters have been taken from the manufacturer's manual. Then, the pose of both the devices have been calculated using the forward kinematics relationship [21]. To map the (x, y, z) coordinates

TABLE I: DH parameters of Geomagic haptic device

Link (i)	θ_i (Joint limits (deg.))	d_i (m)	a_i (m)	α_i (rad)
1	$\theta_1(-56, +56)$	0	0	$-\pi/2$
2	$\theta_2(0, 100)$	0	0.1334	0
3	$\theta_3(47, 69)$	-0.1334	0	$-\pi/2$
4	$\theta_4(-141, 148)$	0	0	$\pi/2$
5	$\theta_5(-87, +57)$	0	0	$-\pi/2$
6	$\theta_6(-150, +150)$	0	0	π

of pose, velocity level mapping is applied to map the whole workspace of the UR5 robot at the remote site, enabling the doctor to scan the wide region of the human body. In this mapping, first, the velocity of the geomagic stylus has been computed using the following relationship.

$$\boldsymbol{v}^g = \frac{\alpha_v}{dt}\left(\begin{bmatrix} x^g(t) \\ y^g(t) \\ z^g(t) \end{bmatrix} + \begin{bmatrix} -1 & 0 & 0 \\ 0 & -1 & 0 \\ 0 & 0 & -1 \end{bmatrix} \begin{bmatrix} x^g(t-1) \\ y^g(t-1) \\ z^g(t-1) \end{bmatrix} \right) \tag{1}$$

where, $[x^g,\, y^g,\, z^g] = \boldsymbol{p}^g$ represents the position coordinates of geomagic stylus, and t is the time instant. The scaling factor (α_v) helps in controlling the speed of the UR5 robot. The time delay in teleoperation will be inversely proportional to this scaling factor. Then, the robot position coordinates $\boldsymbol{p^r}$ are calculated using the following equation.

$$\boldsymbol{p}_t^r = \begin{bmatrix} x^r(t) \\ y^r(t) \\ z^r(t) \end{bmatrix} = \begin{bmatrix} x^r(t-1) \\ y^r(t-1) \\ z^r(t-1) \end{bmatrix} + \boldsymbol{v}^g * dt \tag{2}$$

Due to the structural differences, the one-to-one mapping at orientation level is not a feasible solution and it requires appropriate scaling and offset factors, as given in the relationship below:

$$\boldsymbol{o}_t^r = \begin{bmatrix} \phi^r(t) \\ \theta^r(t) \\ \psi^r(t) \end{bmatrix} = \begin{bmatrix} \alpha_\phi & 0 & 0 \\ 0 & \alpha_\theta & 0 \\ 0 & 0 & \alpha_\psi \end{bmatrix} \begin{bmatrix} \phi^g(t) \\ \theta^g(t) \\ \psi^g(t) \end{bmatrix} \pm \begin{bmatrix} \delta_\phi \\ \delta_\theta \\ \delta_\psi \end{bmatrix} \tag{3}$$

where ϕ, θ and ψ represents the roll, pitch and yaw angles, respectively. α_* and δ_* represent the scaling and offset factors, respectively, in their corresponding orientation ($*$).

The mapping also requires filtering of haptic device signals as it is difficult for humans to move the stylus smoothly without any jitter. Usually, the low-frequency domain represents the useful information of teleoperated device and the high-frequency regions represent the noises. It has been concluded in [22] that position tracking up to 2Hz is necessary for teleoperation of the haptic device while frequencies above that should be suppressed. To realize these requirements of teleoperation, we have implemented a low-pass Butterworth filter with a cutoff frequency of 2Hz at -3dB of pass band.

B. Force control

The force control of the robot is essential to handle contact events in physical human-robot interaction (pHRI) tasks. Robotic ultrasound is one such medical application involving pHRI in an unstructured environment, where a pure motion control strategy will not work. Further, the ultrasound examination requires a varying magnitude of forces for an accurate diagnosis. Thus, the robot should follow precise force-controlled trajectories along the surface of the human body. This is extremely necessary for remote ultrasound systems where the safety of humans is an essential element to consider.

The most commonly used force control approach is impedance control [23], but the selection of impedance parameters to ensure appropriate compliant behaviour in contact, might result in inappropriate trajectory tracking [24].

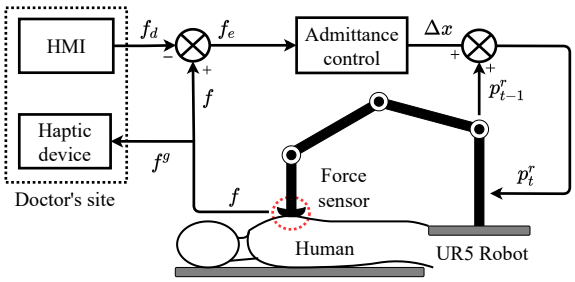

Fig. 5: Force control loop diagram

To solve this problem, we employed an admittance control [25], which produces the desired motion through a predefined relationship with measured force, as shown in Fig. 5. This dynamic relationship is quantified by three parameters i.e. desired Inertia ($\boldsymbol{M_d}$), Damping ($\boldsymbol{B_d}$), and Stiffness ($\boldsymbol{K_d}$), as given in eq. (4).

$$\boldsymbol{M_d}\Delta\ddot{\boldsymbol{x}} + \boldsymbol{B_d}\Delta\dot{\boldsymbol{x}} + \boldsymbol{K_d}\Delta\boldsymbol{x} = \boldsymbol{f}(t) \tag{4}$$

where $\Delta\boldsymbol{x} = \boldsymbol{p}^r - \boldsymbol{p}_d^r$ is the difference between actual and desired position vector of robot, $\boldsymbol{f}$(t) is the measured force vector at probe contact point. In a practical sampling system, the following equations can be employed to compute $\Delta\boldsymbol{x}$:

$$\Delta\dot{\boldsymbol{x}}(t) = (\Delta\boldsymbol{x}(t) - \Delta\boldsymbol{x}(t-1))/T_s \tag{5}$$

$$\Delta\ddot{\boldsymbol{x}}(t) = (\Delta\dot{\boldsymbol{x}}(t) - \Delta\dot{\boldsymbol{x}}(t-1))/T_s \tag{6}$$

where T_s refers to the sampling period. Substituting the above into eq. (4), $\Delta\boldsymbol{x}(t)$ can be calculated online as

$$\Delta\boldsymbol{x}(t) = \frac{\begin{array}{c}\boldsymbol{f}_e(t)T_s^2 + \boldsymbol{B}_d T_s \Delta\boldsymbol{x}(t-1) \\ + \boldsymbol{M}_d(2\Delta\boldsymbol{x}(t-1) - \Delta\boldsymbol{x}(t-2))\end{array}}{\boldsymbol{M}_d + \boldsymbol{B}_d T_s + \boldsymbol{K}_d T_s^2} \tag{7}$$

The position of the robot is then corrected using the error $\Delta\boldsymbol{x}$ which ensures the desired force at the contact point. In addition, the force realized at robot's end-effector is scaled-down and fed back to the haptic device at the doctor's site.

IV. Results and Discussions

In this section, the performance of TR-US has been analyzed to precisely control the fine movements of the probe at the remote site and generate images of diagnostic quality. While various ultrasound examinations can be conducted using this system, we assessed its feasibility using sophisticated abdominal ultrasound, including diagnosis of several organs like liver, kidneys, bladders and spleen. A feasibility study involving 21 human volunteers was conducted at AIIMS between March and May 2021. All volunteers were males with a mean age of 37.09 ± 9.69 years. The Ethics Committee of AIIMS has approved this study (Ref. No. IEC-855). The written informed consent was taken from the volunteers. The system's ability to acquire diagnosable images of abdominal organs was evaluated and the results were compared to the images obtained from the conventional hand-guidance of the probe, referred to as Manual Ultrasound (M-US) in this section. The volunteers and doctors were requested to fill the questionnaire survey to assess the overall perceived efficacy and acceptability of the proposed system.

A. Motion mapping analysis

To verify the effectiveness of the designed filter for suppressing the vibrations in sonographer's hand motion, the velocity of the stylus in x- and y-direction with and without filter is illustrated in Fig. 6. The plots show that the noise has been completely removed, which will enable the doctor to control the probe motion with more precision. Later on,

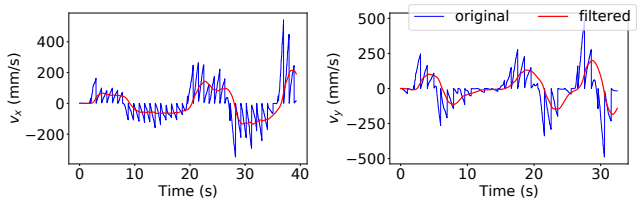

Fig. 6: Haptic device's velocity with and without filtering

the accuracy of mapped motion is verified by comparing the filtered velocity in x- and y-direction and orientations (ϕ, θ, ψ) of geomagic stylus to the robot's end-effector as shown in Fig. 7. The constant values used in eq. (1) and (3)

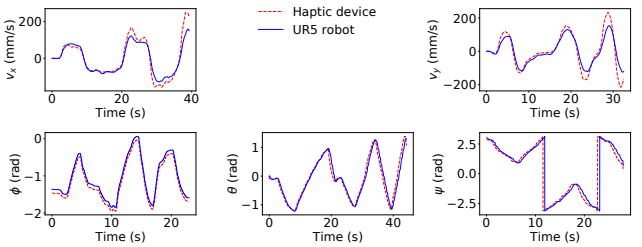

Fig. 7: Motion mapping of haptic device and UR5 robot

to realize this mapping are $\alpha_v = 2$, $\alpha_\theta = \alpha_\phi = -1, \alpha_\psi = 1, \delta_\theta = 1.5, \delta_\phi = \delta_\psi = 0$. The plots show that the robot's end-effector is able to replicate the guided motion accurately.

B. Force tracking analysis

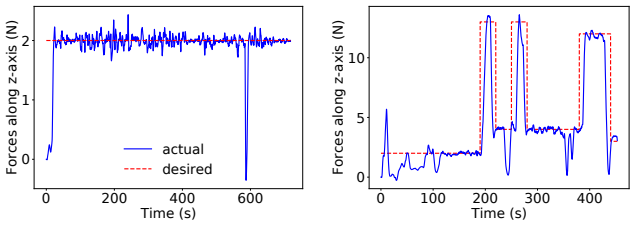

(a) (b)

Fig. 8: Force tracking during ultrasound examination when force is (a) kept constant at 2N (b) varied between $0 - 15$N

To ensure accurate force control, the parameters of admittance controller described in section III-B have been tuned and their values have been taken as $M_d = 1$ Kg, $B_d = 9500$ N-s/m and $K_d = 500000$ N/m. The desired contact force is set as 2N by default; however, the doctor can vary this magnitude of force using the slider given on the HMI. The force values during the two examinations are shown in Fig. 8a and 8b, which shows the system's ability to converge to the variable desired force and stay within safe limits (0-20N).

C. Ultrasound image assessment

All volunteers included in the study have been initially scanned using the M-US system, according to standard abdominal imaging protocol. Immediately after this examination, the same sonographer scanned each volunteer using the TR-US system. Fig. 9 shows the images from both the modalities for one of the volunteers. To compare the quality of images, a senior radiologist has been asked to classify all images as adequate (score=1) or inadequate (score=0) for evaluation. To keep his judgment unbiased, he was blinded to the imaging modality. The radiologist reported adequate TR-US images in the case of liver (17/21), RK (13/21), LK (14/21) and spleen (13/21), while significant reservations were reported for GB (11/21) and UB (10/21). In order to statistically evaluate the comparison to M-US images, a paired sample t-test was carried out, as given in Table II, where a significance threshold of $P < 0.05$ was used.

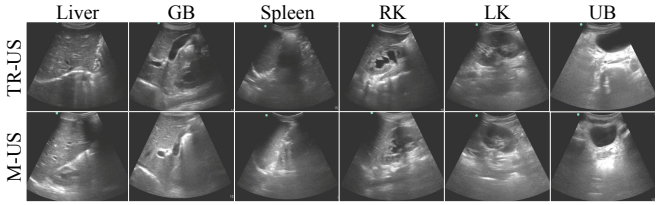

Fig. 9: Comparison of images of Liver, Gall bladder (GB), Spleen, Right Kidney (RK), Left Kidney (LK) and Urinary Bladder (UB) acquired using TR-US and M-US

TABLE II: Statistical differences between TR-US and M-US

Organ	Mean ± Standard deviation score		P-value
	TR-US	M-US	
Liver	0.81 ± 0.40	0.90 ± 0.30	0.1623
Gall Bladder	0.52 ± 0.51	1.00 ± 0.00	0.0004
Right Kidney	0.62 ± 0.50	0.76 ± 0.44	0.0828
Left Kidney	0.67 ± 0.48	0.86 ± 0.36	0.0423
Spleen	0.62 ± 0.50	0.76 ± 0.44	0.0828
Urinary Bladder	0.48 ± 0.51	0.90 ± 0.30	0.0009

The diagnosis of the liver (P=0.1623), RK (P=0.0828), LK (P=0.0423) and spleen (P=0.0828) performed quite well and showed no significant difference. The kidneys and the spleen often lie near the singular configurations of the robot, making it difficult for sonographers to position the probe appropriately. However, this situation has been avoided later when the patient was asked to tilt slightly towards the robot side. The evaluation of the GB (P=0.0004) and UB (P=0.0009) reported a significant difference. This is due to the need for finer probe orientations to focus on these organs, which less-trained doctors are unable to do. In most of the organs, the initial examinations by TR-US were reported inadequate, but later studies report significant improvement in the quality of images. This improvement can be attributed to the learning curve required for the sonographer to get accustomed to the system. In addition, four pathological findings were also identified using TR-US, as shown in Fig. 10, which makes it a suitable alternative for ultrasound-guided procedures like aspiration of ascites, biopsy, etc.

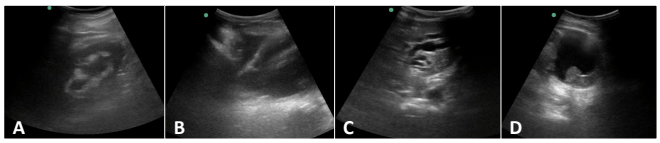

Fig. 10: Pathologies identified: A-hydronephrosis, B-ascites, C-dilated intrahepatic biliary radicles, D-solid cystic mass

The *mean time duration* of TR-US abdominal examination was 19.09 minutes (range 15-27 minutes) compared to 11.14 minutes (range 9-12 minutes) for M-US examinations. However, the duration of the examinations decreased significantly (-14%) from the first 6 to the last 15 examinations.

D. Doctors' and Volunteers' assessment

The various assessments have been carried out to evaluate the system's acceptability and efficacy. First, the NASA Task Load Index (NASA-TLX) based assessment is performed on doctors after each examination. They were asked to answer the standard NASA-TLX based questionnaire for the following parameters: Mental Demand (MD). Physical Demand (PD), Performance (P), Effort (E) and Frustration (F) of the system on a 20-point Likert Scale (i.e. very low=1, very high=20). The results for NASA-TLX assessment are given in Fig. 11a, which shows gradual improvement in the scores of parameters. In order to better visualize this improvement, we have compared the mean score of parameters for the 1-10 and 11-21 trials, as shown in Fig. 11b. The somewhat high score of MD and E parameter can be attributable to sonographers' lack of competence with the technology. The significant improvement in PD (-46%) and P (+28%) parameter is due to the interactive force modulation, which does not cause M-US like physical strain on the muscles of sonographers. Across all trials, the enthusiasm for using a new technology resulted in a low degree of frustration.

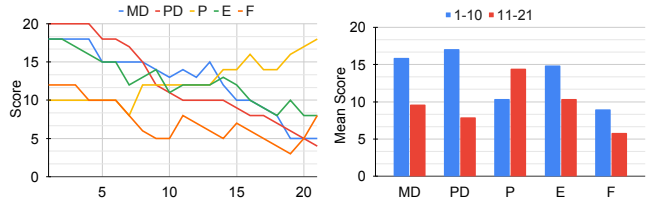

(a) (b)

Fig. 11: NASA-TLX results. (a) Variation of parameters' score over each trial (b) Comparison of mean value of parameters' score for 1-10 and 11-21 trials

Furthermore, in order to evaluate the overall acceptability of the system, the doctors and volunteers were requested to rate our self-designed task-specific questionnaire survey on a standard 5-point Likert scale (Strongly disagree, Disagree, Neutral, Agree, Strongly agree). The results for the survey are shown in Fig. 12. The doctors agreed that the system is easy to operate and capable of acquiring good quality images. Doctors experienced difficulties operating the robot for the initial trials, but with more training, they became habituated to the probe motions. Overall, the doctors rated the system between 5-8 (average=6.38) out of 10. The volunteers showed acceptance towards the technology and felt a slight difference between the M-US and TR-US procedures. The majority of them felt less pressure on their body than M-US and were comfortable during the procedure. They agreed to trust the results of this technology, knowing that doctor is in the loop and controlling the US probe. Overall, the system was rated between 5-8 (average=6.2) by volunteers.

In order to test the reliability of our self-designed questionnaire, we evaluated the value of *Cronbach's Alpha* (reliability index), which is found to be 0.948 for doctors' and 0.958 for volunteers' questionnaire. The closer this index's value is to 1, the better the number of different items (questions) tells us about the system's characteristics under evaluation.

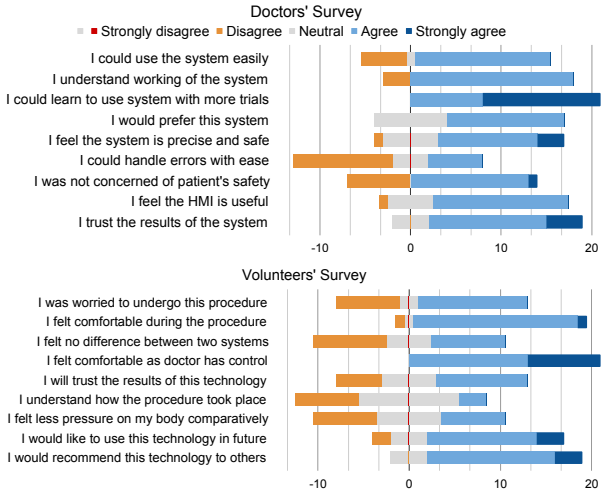

Fig. 12: Results of questionnaire survey based on 5-point Likert scale. Diverging bar-chart is used to better visualize the positive and negative feedback.

V. Conclusion

A Telerobotic Ultrasound (TR-US) system has been proposed in this paper for remote US imaging of abdomen organs to ensure the safety of doctors during the COVID-19 pandemic. The system provides a precise platform for comprehensive control and perception of all components of the manual procedure. The 6D pose of the probe was teleoperated by the doctor while the varying force on the abdomen organs was controlled through the admittance controller and human-machine interface. A comprehensive feasibility study has been performed at AIIMS, Delhi, which shows good imaging quality and high acceptability among volunteers and doctors. The system's primary concern is the need for doctors to undergo training to get comfortable with the movements of teleoperated probe. Our future work will attempt to automate the orientation and force adjustment of the US probe by expanding the scope of breast ultrasound specific controller proposed in [26], [27] to abdomen organs. The optimal design of the probe gripper will also be investigated to maximize the orientation area of the US probe. Finally, we will conduct a large-scale evaluation of the system's performance in long-distance teleoperation.

REFERENCES

[1] Government of India, "Ministry of Family and Health Welfware," https://www.mohfw.gov.in/, 2021, [Online; accessed 01-June-2021].

[2] B. Gates, "Responding to covid-19?a once-in-a-century pandemic?" *New England Journal of Medicine*, vol. 382, no. 18, pp. 1677–1679, 2020.

[3] G. Soldati, A. Smargiassi, R. Inchingolo, D. Buonsenso, T. Perrone, D. F. Briganti, S. Perlini, E. Torri, A. Mariani, E. E. Mossolani *et al.*, "Proposal for international standardization of the use of lung ultrasound for covid-19 patients; a simple, quantitative, reproducible method," *J ultrasound Med*, vol. 10, 2020.

[4] ——, "Is there a role for lung ultrasound during the covid-19 pandemic?" *Journal of Ultrasound in Medicine*, 2020.

[5] O. Y. Antúnez-Montes and D. Buonsenso, "Routine use of point-of-care lung ultrasound during the covid-19 pandemic," *Medicina intensiva*, 2020.

[6] T. C. COVID *et al.*, "Characteristics of health care personnel with covid-19-united states, february 12-april 9, 2020." 2020.

[7] M. Tavakoli, J. Carriere, and A. Torabi, "Robotics, smart wearable technologies, and autonomous intelligent systems for healthcare during the covid-19 pandemic: An analysis of the state of the art and future vision," *Advanced Intelligent Systems*, vol. 2, no. 7, p. 2000071, 2020.

[8] F. von Haxthausen, S. Böttger, D. Wulff, J. Hagenah, V. García-Vázquez, and S. Ipsen, "Medical robotics for ultrasound imaging: current systems and future trends," *Current Robotics Reports*, pp. 1–17, 2021.

[9] R. Monfaredi, E. Wilson, B. Azizi koutenaei, B. Labrecque, K. Leroy, J. Goldie, E. Louis, D. Swerdlow, and K. Cleary, "Robot-assisted ultrasound imaging: Overview and development of a parallel telerobotic system," *Minimally Invasive Therapy & Allied Technologies*, vol. 24, no. 1, pp. 54–62, 2015.

[10] X. Guan, H. Wu, X. Hou, Q. Teng, S. Wei, T. Jiang, J. Zhang, B. Wang, J. Yang, and L. Xiong, "Study of a 6dof robot assisted ultrasound scanning system and its simulated control handle," in *2017 IEEE International Conference on Cybernetics and Intelligent Systems (CIS) and IEEE Conference on Robotics, Automation and Mechatronics (RAM)*. IEEE, 2017, pp. 469–474.

[11] K. Mathiassen, J. E. Fjellin, K. Glette, P. K. Hol, and O. J. Elle, "An ultrasound robotic system using the commercial robot ur5," *Frontiers in Robotics and AI*, vol. 3, p. 1, 2016.

[12] P. Arbeille, K. Zuj, A. Saccomandi, J. Ruiz, E. Andre, C. de la Porte, G. Carles, J. Blouin, and M. Georgescu, "Teleoperated echograph and probe transducer for remote ultrasound investigation on isolated patients (study of 100 cases)," *TELEMEDICINE and e-HEALTH*, vol. 22, no. 7, pp. 599–607, 2016.

[13] P. Arbeille, D. Chaput, K. Zuj, A. Depriester, A. Maillet, O. Belbis, P. Benarroche, and S. Barde, "Remote echography between a ground control center and the international space station using a tele-operated echograph with motorized probe," *Ultrasound in medicine & biology*, vol. 44, no. 11, pp. 2406–2412, 2018.

[14] J. Wang, C. Peng, Y. Zhao, R. Ye, J. Hong, H. Huang, and L. Chen, "Application of a robotic tele-echography system for covid-19 pneumonia," *Journal of Ultrasound in Medicine*, vol. 40, no. 2, pp. 385–390, 2021.

[15] S. Wu, K. Li, R. Ye, Y. Lu, J. Xu, L. Xiong, A. Cui, Y. Li, C. Peng, and F. Lv, "Robot-assisted teleultrasound assessment of cardiopulmonary function on a patient with confirmed covid-19 in a cabin hospital," *Advanced Ultrasound in Diagnosis and Therapy*, vol. 4, no. 2, pp. 128–130, 2020.

[16] S. Avgousti, A. S. Panayides, A. P. Jossif, E. G. Christoforou, P. Vieyres, C. Novales, S. Voskarides, and C. S. Pattichis, "Cardiac ultrasonography over 4g wireless networks using a tele-operated robot," *Healthcare technology letters*, vol. 3, no. 3, pp. 212–217, 2016.

[17] M. Georgescu, A. Sacccomandi, B. Baudron, and P. L. Arbeille, "Remote sonography in routine clinical practice between two isolated medical centers and the university hospital using a robotic arm: a 1-year study," *Telemedicine and e-Health*, vol. 22, no. 4, pp. 276–281, 2016.

[18] S. J. Adams, B. E. Burbridge, A. Badea, L. Langford, V. Vergara, R. Bryce, L. Bustamante, I. M. Mendez, and P. S. Babyn, "Initial experience using a telerobotic ultrasound system for adult abdominal sonography," *Canadian Association of Radiologists' Journal*, vol. 68, no. 3, pp. 308–314, 2017.

[19] S. J. Adams, B. Burbridge, H. Obaid, G. Stoneham, P. Babyn, and I. Mendez, "Telerobotic sonography for remote diagnostic imaging: Narrative review of current developments and clinical applications," *Journal of Ultrasound in Medicine*, 2020.

[20] Z. Chen, S. Yan, M. Yuan, B. Yao, and J. Hu, "Modular development of master-slave asymmetric teleoperation systems with a novel workspace mapping algorithm," *IEEE Access*, vol. 6, pp. 15 356–15 364, 2018.

[21] S. K. Saha, *Introduction to robotics*. Tata McGraw-Hill Education, 2014.

[22] C. Zandsteeg, D. Bruijnen, and M. Van de Molengraft, "Haptic teleoperation system control design for the ultrasound task: A loop-shaping approach," *Mechatronics*, vol. 20, no. 7, pp. 767–777, 2010.

[23] N. Hogan, "Impedance control: An approach to manipulation: Part i?theory," 1985.

[24] W. S. Newman, "Stability and performance limits of interaction controllers," 1992.

[25] A. D. Udai and S. K. Saha, "Dynamic simulation of serial robots under force control," *International Journal of Intelligent Machines and Robotics*, vol. 1, no. 1, pp. 79–108, 2018.

[26] J. Carriere, J. Fong, T. Meyer, R. Sloboda, S. Husain, N. Usmani, and M. Tavakoli, "An admittance-controlled robotic assistant for semi-autonomous breast ultrasound scanning," in *2019 International Symposium on Medical Robotics (ISMR)*. IEEE, 2019, pp. 1–7.

[27] M. Akbari, J. Carriere, T. Meyer, R. Sloboda, S. Husain, N. Usmani, and M. Tavakoli, "Robotic ultrasound scanning with real-time image-based force adjustment: Quick response for enabling physical distancing during the covid-19 pandemic," *Frontiers in Robotics and AI*, vol. 8, p. 62, 2021.